

# Upgrading Asphaltenes by Oil Droplets Striking a Charged TiO<sub>2</sub>-Immobilized Paper Surface

Yin-Hung Lai,<sup>†,‡</sup> Zhenpeng Zhou,<sup>†,‡</sup> Chanbasha Basheer,<sup>‡,§</sup> and Richard N. Zare<sup>\*,‡</sup>

<sup>†</sup>Department of Chemistry, Stanford University, Stanford, California 94305, United States

<sup>§</sup>Department of Chemistry, King Fahd University of Petroleum and Minerals, Dhahran 31261, Saudi Arabia

## Supporting Information

**ABSTRACT:** The conversion of heavy oil fractions into lighter oil fractions is highly essential for meeting the growing demand for fuels in continuous depletion of oil reserves and for environmental remediation. We demonstrate an oil degradation approach where oil microdroplets are sprayed in air at room temperature onto untreated TiO<sub>2</sub> nanoparticles-coated filter paper to which we apply an electrical potential. Two model polycyclic aromatic hydrocarbons as well as a crude oil sample show degradation on the microsecond time scale. Heterogeneous catalysis of a biphasic (organic/aqueous) reaction occurs at the interface of microdroplets and the charged TiO<sub>2</sub> surface. The fragmentation yield is increased by cycling the process. The relative fragmentation yield of a model compound (rubrene) increased from 16.9% in the first cycle to 32.6% in the third cycle. This convenient and efficient method suggests possible future industrial applications.

## 1. INTRODUCTION

The main goal of oil upgrading is to break down heavy fractions of crude oil (asphaltenes) into smaller molecules for the development of alternative fuels and to facilitate oil recovery.<sup>1–4</sup> Development of alternative fuels is a promising strategy to overcome continuous depletion of conventional oil reserves and to meet the growing demand for fuels.<sup>5,6</sup> Furthermore, oil degradation is also useful for environmental remediation, such as an accidental discharge of oils to water resources, which might pose severe threats to ecological systems.<sup>7,8</sup> However, because of rigid structures, high density, and high viscosity, methods used to break down asphaltenes, such as hydro- and thermal cracking<sup>4</sup> and supercritical fluid processing,<sup>9</sup> are required to act at elevated temperatures and pressures.

The development of nanoparticles as catalysts to improve the degradation efficiency of heavy oil has received much interest.<sup>1,4,10–12</sup> Photocatalytic degradation using titanium dioxide (TiO<sub>2</sub>) is one of the most promising methods because of its low cost and environmental friendliness.<sup>13</sup> Extensive efforts have been devoted to improving the photocatalytic efficiency of TiO<sub>2</sub>, such as modifications to reduce the band gap<sup>14,15</sup> and increase reactivity<sup>16</sup> and nanofabrication to enlarge the surface/volume ratio.<sup>17</sup> Degradation of asphaltenes still only takes place in strongly acidic or basic environments in reactors, even with the presence of TiO<sub>2</sub> plus intense ultraviolet (UV) irradiation.<sup>10,18</sup> Moreover, photocatalytic degradation normally takes minutes to days.<sup>19–22</sup> These factors lead to difficulty in scaling up for industrial use. A low-cost, rapid, and environmentally friendly alternative is urgently needed for oil upgrading.

We report a new method to expedite the degradation rate of asphaltenes by spraying oil microdroplets onto the charged surface of a filter paper coated with TiO<sub>2</sub> nanoparticles under ambient conditions. In our system, no light is needed; instead, we apply voltage to initiate the heterogeneously catalytic

degradation process. The time scale of degradation is in microseconds. We used a spray source to generate oil microdroplets. This method allows us to conduct degradation reactions on or near the surface of the microdroplets, where acceleration of reaction rates has been reported.<sup>23–25</sup> Sample extracted from the paper is collected with a glass tube and analyzed using our laboratory-built laser desorption/laser ionization mass spectrometry (L<sup>2</sup>MS).<sup>26</sup> L<sup>2</sup>MS, which minimizes the interference from ion–molecule interactions, enables us to probe unknown structures in a complex system. In comparison to conventional chromatography, L<sup>2</sup>MS is capable of resolving individual molecule species for an extended mass range in a single experiment with very little sample handling.<sup>27</sup> Two model compounds, rubrene and hematoporphyrin, which are commonly found in asphaltenes, are studied. We propose an electric-field-induced mechanism for the oil degradation process on the charged surface of a TiO<sub>2</sub>-immobilized filter paper involving the generation of OH radicals. The fragmentation yield is increased by cycling the process, which means to retreat the oil sample that has contacted the charged TiO<sub>2</sub>-coated paper. Finally, proof of concept was shown for this method by degrading a crude oil sample without dilution.

## 2. MATERIALS AND METHODS

**2.1. Reagents.** Rubrene, hematoporphyrin, and TiO<sub>2</sub> (anatase, <25 nm particle size) were purchased from Sigma-Aldrich (Milwaukee, WI, U.S.A.). Filter papers of fine porosity (grade P2) were purchased from Fisher Scientific (Nepean, Ontario, Canada). A crude oil sample, Arabian Heavy crude oil, was obtained from Prof. Abdullah Sultan, King Fahd University of Petroleum and Minerals, Saudi Arabia. The specifications of the crude oil sample, such as American Petroleum Institute (API) gravity and density, are provided in section D of the Supporting Information. Rubrene and hematoporphyrin were

Received: August 8, 2017

Revised: October 5, 2017

Published: October 12, 2017

dissolved in toluene/isopropyl alcohol (1:1, v/v) to a concentration of 0.02 mg/mL. Both diluted and undiluted crude oil samples were examined. We diluted crude oil samples to 1:400 in toluene (v/v). TiO<sub>2</sub> was dispersed in distilled water to a concentration of 2.5 mg/mL.

**2.2. Workflow for the Heterogeneously Catalytic Degradation of Asphaltenes on the Surface of the TiO<sub>2</sub>-Immobilized Paper.** Oil sample microdroplets were sprayed onto an aqueous wet paper surface coated with TiO<sub>2</sub> nanoparticles inside a glass tube. The reaction system is a heterogeneous catalysis (TiO<sub>2</sub> nanoparticles/liquid samples) of a biphasic solvent system (organic/aqueous). TiO<sub>2</sub> nanoparticles were immobilized on a filter paper using the dip-coating method.<sup>28</sup> Briefly, a triangle-shaped filter paper was coated by dipping it into a suspension of aqueous TiO<sub>2</sub> solution and sonicated for 1 min. Thereafter, the paper containing the TiO<sub>2</sub> nanoparticle was removed from the suspension of aqueous TiO<sub>2</sub>. The back end of the TiO<sub>2</sub>-coated filter paper was then held using a steel alligator clip. A voltage of +2 kV was applied to the wet TiO<sub>2</sub>-coated filter paper. A volume of 500  $\mu$ L of oil sample solution in a glass syringe was infused into a fused-silica capillary (100  $\mu$ m inner diameter and 350  $\mu$ m outer diameter) using a syringe pump at a flow rate of 25  $\mu$ L/min. Compressed air was used as the nebulizing gas, and the pressure was regulated at 60 psi to facilitate the generation of microdroplets. After the treatment, 500  $\mu$ L of toluene/isopropyl alcohol (1:1, v/v) solvent mixture was used to extract the sample from the filter paper for the mass spectrometric analysis. The recovery rate of the extracted sample from the paper is 69% using this method. Notably, high voltage was only applied to the paper that carried TiO<sub>2</sub>. For control experiments, model compounds were directly analyzed without the treatment of heterogeneous catalysis.

**2.3. Mass Spectrometric Analysis.** Detection of asphaltenes by L<sup>2</sup>MS has been reported elsewhere.<sup>26,29</sup> Briefly, the sample solution was deposited and air-dried on a glass platter. The glass platter was transferred to a high-vacuum chamber ( $5 \times 10^{-8}$  Torr). Desorption and ionization in L<sup>2</sup>MS were separately optimized, in both time and space. A pulsed CO<sub>2</sub> laser of  $\lambda = 10.6 \mu$ m was first introduced to desorb samples (ALLMARK APS, ALLTEC GmbH, Selmsdorf, Germany). The CO<sub>2</sub> laser beam was focused by an objective to a circular spot of 50  $\mu$ m in diameter. Because the photon energy of the CO<sub>2</sub> laser is about 2 orders of magnitude lower than the ionization potential of samples,<sup>30</sup> it only serves desorption of neutral molecules. Following a time delay of 40  $\mu$ s, desorbed neutral molecules were ionized by irradiating a pulsed F<sub>2</sub> excimer laser of  $\lambda = 157$  nm via 1 + 1 resonance-enhanced multiphoton ionization (ExciStar XS 200, Coherent, Santa Clara, CA, U.S.A.). The ionized sample was analyzed by a laboratory-built Wiley–McLaren-type time-of-flight mass spectrometer. Energies of desorption and ionization lasers were fixed through the entire experiment. A mass spectrum of every spot was the average over 20 laser shots at random position on the surface. The magnitude of the signal was increased using an amplifier (model 474, Ortec, Oak Ridge, TN, U.S.A.) and recorded by a digital oscilloscope (LT342, LeCroy, Chestnut Ridge, NY, U.S.A.). Molecular structures of selected fragments by the heterogeneously catalytic degradation were predicted using collision-induced dissociation (CID) in a LTQ-Orbitrap XL (Thermo Fisher Scientific, Waltham, MA, U.S.A.).

### 3. RESULTS AND DISCUSSION

**3.1. Electric-Field-Induced Degradation of Asphaltenes Using TiO<sub>2</sub>-Coated Filter Paper.** Figure 1 shows the experimental setup. A spray source is loaded with an oil sample. The oil sample is infused into a capillary with a syringe pump at an optimized flow rate. Sheath gas of compressed air is used to facilitate the atomization. The oil sample is sprayed onto TiO<sub>2</sub> nanoparticles (<25 nm in diameter) immobilized filter paper placed inside a glass tube. We used filter paper as the simplest choice, which has proven to be a useful and robust material for down-sizing and simplifying analytical chemistry.<sup>31,32</sup> Anatase TiO<sub>2</sub> nanoparticles are used without any pretreatment. The off-line method allows us to treat oil *in situ* and does not require us

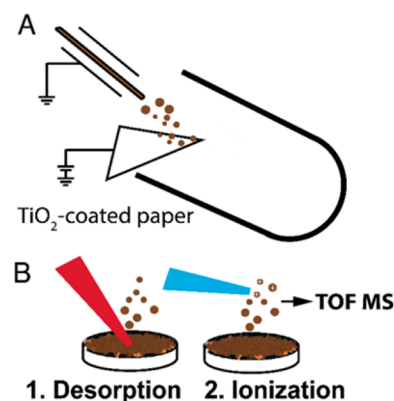


**Figure 1.** Workflow for studying heterogeneously catalytic degradation of asphaltenes on the surface of TiO<sub>2</sub>-containing paper with a biphasic solvent system (organic/aqueous). (A) Spray source is used to accommodate sample solution (organic solution, in brown color), which sprays sample microdroplets onto the aqueous wet surface of the filter paper containing anatase TiO<sub>2</sub> nanoparticles. The spray source of sample solution is electrically grounded. High voltage (+2 kV) is applied to the wet paper coated with TiO<sub>2</sub> nanoparticles. (B) Extracted sample is deposited on a glass platter and analyzed using L<sup>2</sup>MS. For further details, please refer to the main text.

to place the detection system immediately after the degradation treatment. Following treatment, we extracted the sample from the paper with solvent and used L<sup>2</sup>MS to analyze the products. In contrast to conventional laser desorption/ionization (LDI) mass spectrometry, L<sup>2</sup>MS minimizes interferences from ion–molecule interactions from matrices and enables us to probe the molecular architecture of complex aliphatic and aromatic hydrocarbons.<sup>26</sup> The polycyclic aromatic hydrocarbon (PAH), rubrene, and the nitrogen-containing aromatic compound, hematoporphyrin, were selected as model compounds because these compounds are thought to resemble asphaltenes.<sup>33</sup> As shown in panels b and d of Figure 2, these two model

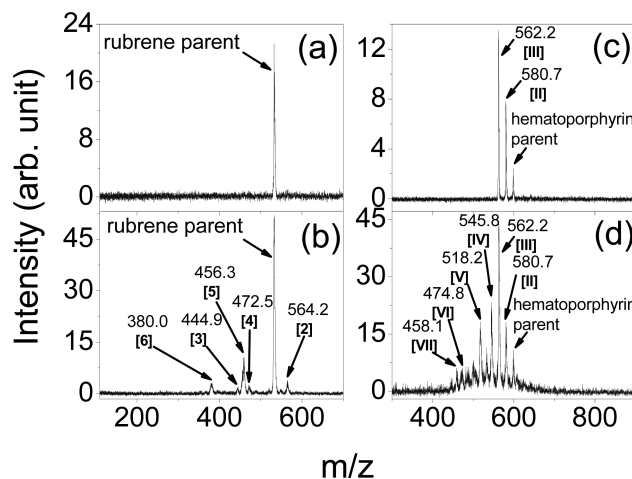
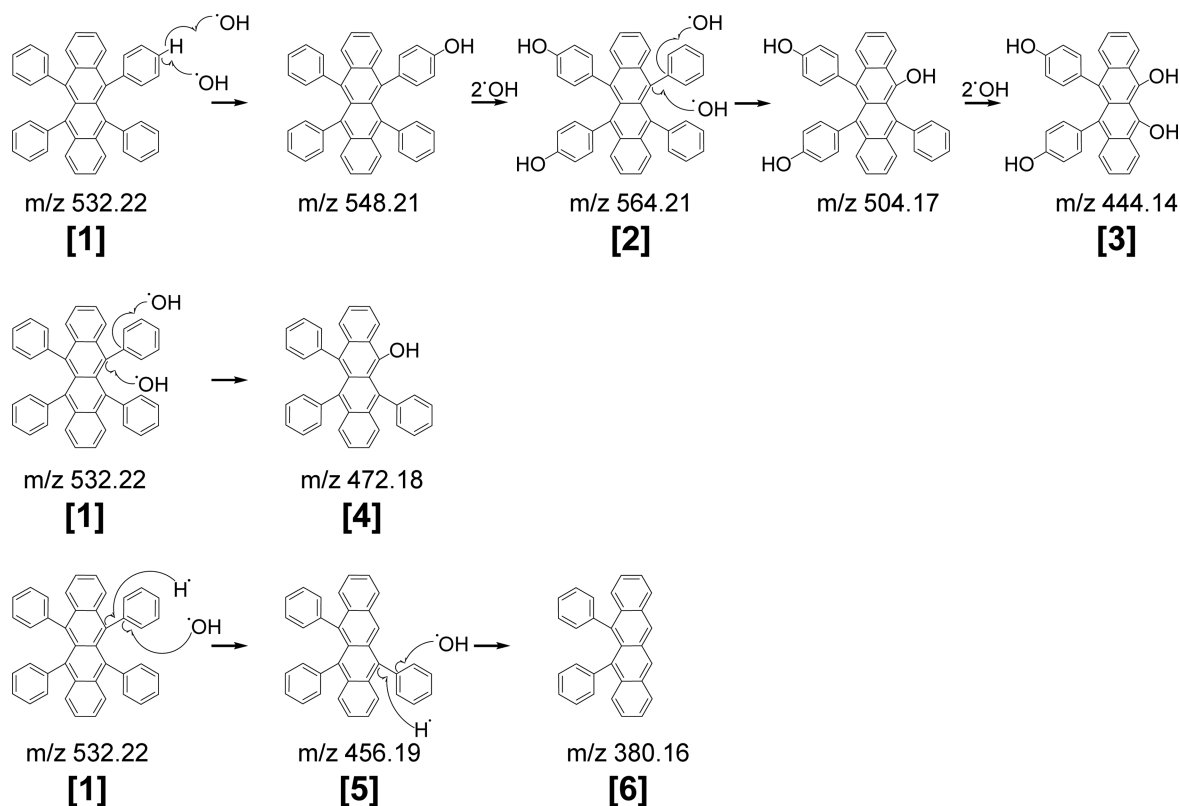


**Figure 2.** L<sup>2</sup>MS mass spectra of control and TiO<sub>2</sub>-catalyzed degradation of PAHs: (a) rubrene control, (c) hematoporphyrin control, and TiO<sub>2</sub>-catalyzed degradation products of (b) rubrene and (d) hematoporphyrin. In panel b, structures for the fragments 2–6 are given in Scheme 1. In panels c and d, II and III correspond to the loss from the parent of one and two water molecules. For more details on degradation pathways and peak identification of fragments III–VII in panel d, please see the main text and sections A and B of the Supporting Information.

Scheme 1. Postulated Degradation Pathway of Rubrene Involving Hydroxyl Radicals



compounds reacted with the functionalized catalysts to which an electrical potential is applied to generate new peaks. We will propose a degradation pathway in the next section and predict chemical compositions of new peaks after heterogeneous catalysis of rubrene and hematoporphyrin. In sharp contrast, only the parent ion was detected in control experiments for rubrene (Figure 2a). In the control experiment of hematoporphyrin (Figure 2c), besides the parent ion, two peaks (II and III) corresponding to the loss of 1–2 units of water also appear in the spectrum. We do not observe any product from solvent (toluene and isopropyl alcohol). We have tried to degrade compact acenes, including pyrene, coronene, 2-ethylanthracene, and 1-phenylanthracene. However, with our method, these acenes cannot be degraded. We suppose that it is because compact aromatic structures are too energetically stable to be degraded.

**3.2. Proposed Mechanism for Asphaltene Microdroplet Degradation on a Charged Surface Containing TiO<sub>2</sub> Nanoparticles.** We used electric-field-induced TiO<sub>2</sub> for asphaltene degradation on the surface of charged TiO<sub>2</sub>-coated paper. Unlike conventional photocatalysis,<sup>34,35</sup> light is not needed in our system. Instead, high voltage was applied to the paper containing TiO<sub>2</sub> nanoparticles to initiate the process. The high electric field charges up the surface and activates TiO<sub>2</sub> to generate electron (e<sup>-</sup>)-hole (h<sup>+</sup>) pairs.



Applied voltage not only determines the sign of the surface charge but also overwhelmingly enhances its magnitude.<sup>36</sup> Herein, holes were preferentially selected by applying positive 2 kV because the oxidizing power of holes is significantly stronger than the reducing power of electrons.<sup>37</sup> Most importantly, the recombination of e<sup>-</sup>-h<sup>+</sup> pairs can be suppressed, because

electrons are abstracted by the positive voltage.<sup>38</sup> Highly oxidative holes (h<sup>+</sup>) near the surface split adsorbed water molecules and form hydroxyl radicals (OH<sup>•</sup>).



Hydroxyl radicals react with hydrocarbons when sample microdroplets strike the TiO<sub>2</sub> surface. On the basis of the experimental observation, the postulated hydroxyl-radical-involved degradation pathway of rubrene is proposed in Scheme 1. To verify the involvement of hydroxyl radicals in degradation,<sup>37</sup> a TiO<sub>2</sub>-catalyzed rubrene species (2) was selected to conduct the structural identification using a high-resolution Orbitrap mass spectrometer combined with CID. In tandem mass spectrometry (MS/MS) by CID, product ions that correspond to loss of water, cleavages of benzene rings, and their combinations were observed to facilitate the structural prediction. Importantly, water loss from [2 + H]<sup>+</sup> (*m/z* 565.21) in the positive CID analysis (Figure S2 of the Supporting Information) indicates the existence of an -OH group, which shows the involvement of hydroxyl radicals in the degradation of rubrene. For pristine rubrene, it is composed of only carbons and hydrogens. A postulated hydroxyl-radical-involved degradation pathway for hematoporphyrin was provided in Scheme S1 of the Supporting Information.

The following control experiments using rubrene were conducted to better understand the degradation process: (1) with uncoated filter paper plus high voltage and (2) with electrically grounded TiO<sub>2</sub>-immobilized filter paper. None of the control studies showed degradation of rubrene. Furthermore, a control experiment was conducted by applying a negative voltage (-2 kV). Under the negative voltage condition, positive holes were presumably suppressed and, therefore, OH radicals were also suppressed. This result of no

degradation supports the proposed mechanism involving degradation by hydroxyl radicals. Interestingly, we also deposited sample solution through a micropipette on TiO<sub>2</sub>-immobilized filter paper and then applied +2 kV to it for 20 min. The extracted sample showed no degradation of rubrene. These control experiments indicate that microdroplets play an essential role in the degradation process and reinforce the important role of interfacial chemistry in causing the chemical transformation.<sup>39</sup>

Degradation occurs at the interface of the sample droplets upon striking the surface of the TiO<sub>2</sub>-coated paper. When compared to the bulk solution, more interfacial area is created in microdroplets, owing to their large surface/volume ratios. Furthermore, by immobilizing the TiO<sub>2</sub> nanoparticles, we avoid the difficulty in separating the catalyst from the reaction media. Moreover, the same TiO<sub>2</sub>-embedded support can be easily reused over several cycles. As shown in Figure 3, the relative

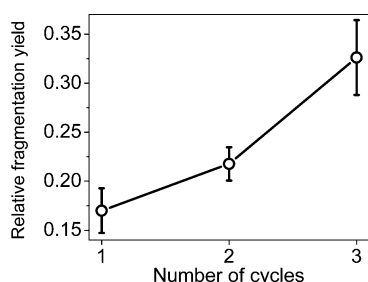


**Figure 3.** Relative fragmentation yield of rubrene as a function of the cycling number of the process. Error bars represent one standard deviation of triplicate measurements.

fragmentation yield of rubrene is further increased by recycling the process, that is, by collecting the treated oil sample and respraying it onto the TiO<sub>2</sub>-coated paper. In Figure 3, intensities of all fragmented peaks of rubrene were summed up and divided by the total ion intensities to obtain the relative fragmentation yield. In the first cycle, a 16.9% relative fragmentation yield was obtained. During the third cycle, a 32.6% relative fragmentation yield was achieved. The degradation reaction occurs in an organic/aqueous biphasic system. Surfactants are typically added to the reaction solution to increase sample miscibility and interfacial surface area.<sup>40,41</sup>

However, a serious drawback is that surfactants can be difficult to separate from the final products. Please note that our method has been conducted without using surfactants.

**3.3. Time Scale and Factors Affecting the Accelerated Degradation Processes.** The present study shows that the degradation on the charged TiO<sub>2</sub>-immobilized paper occurs on the microsecond time scale, because degradation competes with charge-carrier recombination and lifetimes of surface charges.<sup>35,42</sup> Therefore, the reaction time scale has little relationship with contact or mixing time. It is important to consider that new droplets strike paper that has been exposed to other droplets, making the precise time scale discussion difficult. In sharp contrast, photocatalytic degradation of PAHs with TiO<sub>2</sub> normally requires minutes to hours in the bulk phase.<sup>18–20,43–45</sup> More than 1000-fold acceleration of the degradation rate was found for the present method. One might question these arguments as being too good to be true, but striking findings of reaction rate acceleration with microdroplets has been reported many times before. For example, reaction rates of the Hantzsch synthesis of 1,4-dihydropyr-

idines<sup>46</sup> and the Pomeranz–Fritsch synthesis of isoquinoline<sup>47</sup> were increased by more than 5 orders of magnitude in microdroplets. More evidence showing a remarkable acceleration of reaction on the surface of microdroplets was reviewed in a recently published paper.<sup>48</sup>

Some possible reasons accounting for increased degradation rates were discussed. First, electrons from the e<sup>-</sup>-h<sup>+</sup> pairs were abstracted by applying an electric field, and e<sup>-</sup>-h<sup>+</sup> recombination was efficiently suppressed. As a result, the lifetime of the holes is increased, which is akin to the result of charge scavenging,<sup>37</sup> which facilitates subsequent degradation reactions. Second, the enlarged surface/volume ratio enhances reaction possibilities in streamlining degradation processes because those biphasic reactions only occur on the interface.<sup>6</sup> This work is consistent with the previous report that the biphasic reaction was greatly accelerated when carried out in vigorously stirred aqueous suspension, owing to the increase of the area of surface contact.<sup>49</sup> From the energetic point of view, in comparison to the bulk phase, relatively low binding energies of reactants were reported on the droplet interface, which lower reaction barriers and facilitate reactions.<sup>24</sup> These aforementioned factors might cumulatively contribute to the increased degradation rate, but further investigation is needed to evaluate the relative contribution of each factor.

### 3.4. Upgrading Crude Oil under Ambient Conditions.

Figure 4 presents a proof of concept demonstrating the

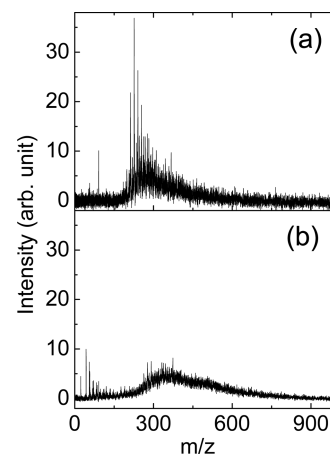


**Figure 4.** Example of oil upgrading. (a) Control in which no treatment is conducted and the oil sample is directly analyzed by L<sup>2</sup>MS. (b) L<sup>2</sup>MS spectrum of an extracted oil sample after striking a paper surface having TiO<sub>2</sub> nanoparticles held at +2 kV.

effectiveness of this technique for upgrading crude oil samples under ambient conditions, that is, room temperature and atmospheric pressure. In the control experiment of the real sample, the distribution of peaks mainly spanned from *m/z* 200 to 400. After TiO<sub>2</sub> catalysis, a new distribution from *m/z* 200 to less than 100 appeared. Both a downward shift to low mass range and an upward shift to high mass range was observed. These higher mass products, which are the result of polymerization, are still soluble in the solvent that we are using, unlike coke. Further analysis is needed for structural identification of these new peaks. We define three mass-range regions to quantify the percentages of downward and upward shifts: (1) *m/z* 0–180, (2) *m/z* 180–550, and (3) *m/z* 550–800. For the control study, 98.9% of total ions are populated in the range of *m/z* 180–550, whereas *m/z* 0–180 and 550–800

have 0.1 and 0.9%, respectively. After heterogeneous catalysis,  $m/z$  0–180 and 550–800 have total ions of 5.9 and 19.4%, respectively. A pie chart displaying populations in these three  $m/z$  regions is provided in section C of the Supporting Information.

Our method works on undiluted crude oil samples. A video was placed in section E of the Supporting Information to show how the experiment proceeds as well as what the contact region looks like. With regard to the video, when oil droplets strike the  $\text{TiO}_2$ -immobilized paper, some droplets are adsorbed on the paper and some splash. Subsequent droplets strike the wet surface, where droplets have already landed. The  $\text{L}^2\text{MS}$  mass spectrum of the treated undiluted crude oil sample is shown in section E of the Supporting Information. The distribution of peaks shifts to the low mass range. The degraded peaks are not as many as those in the diluted crude oil samples. Fragmentation is supposed to be limited by the surface density of activated  $\text{TiO}_2$ , as well as the size of droplets. The undiluted crude oil sample is more viscous and leads to a larger droplet size.

#### 4. CONCLUSION

This study presents a proof-of-concept for oil upgrading involving microdroplet chemistry to enhance the yield of oil degradation. Distinct from the conventional photocatalysis, this degradation process is accomplished without a light source. Two aromatic model PAHs are chemically degraded when sample microdroplets strike a charged paper surface containing  $\text{TiO}_2$  nanoparticles. On the basis of structural measurements of the reacted sample using a high-resolution mass spectrometer combined with CID, a fragmentation pathway involving hydroxyl radicals is proposed. Degradation processes are accomplished on the microsecond time scale, which takes place at the interface between microdroplets and the surface of the  $\text{TiO}_2$ -coated paper. Our method allows for the degradation of crude oil samples at room temperature and atmospheric pressure with little sample preparation. It would be anticipated that the method benefits the oil upgrading and environmental remediation from understanding the processes that break down heavy fractions into smaller molecules. It is also expected that a further engineering development, such as the use of a more robust support, is needed for industrial scaling.

#### ■ ASSOCIATED CONTENT

##### Supporting Information

The Supporting Information is available free of charge on the ACS Publications website at DOI: 10.1021/acs.energyfuels.7b02338.

$\text{L}^2\text{MS}$  mass spectrum of  $\text{TiO}_2$ -catalyzed hematoporphyrin degradation and proposed degradation pathway (section A), CID analysis of selected  $\text{TiO}_2$ -catalyzed hydrocarbons (section B), pie chart of ion populations in three  $m/z$  regions for the control and  $\text{TiO}_2$ -catalyzed degradation of a crude oil sample (section C), specifications of the crude oil sample (section D), and video of the spray of an undiluted crude oil sample and  $\text{L}^2\text{MS}$  mass spectrum of  $\text{TiO}_2$ -catalyzed undiluted crude oil degradation (section E) (PDF)

Video of the spray of an undiluted crude oil sample (MPG)

#### ■ AUTHOR INFORMATION

##### Corresponding Author

\*E-mail: zare@stanford.edu.

##### ORCID

Yin-Hung Lai: 0000-0003-4245-2016

Richard N. Zare: 0000-0001-5266-4253

##### Author Contributions

<sup>†</sup>Yin-Hung Lai and Zhenpeng Zhou contributed equally to this work.

##### Notes

The authors declare no competing financial interest.

#### ■ ACKNOWLEDGMENTS

This work was supported by the Air Force Office of Scientific Research through the Basic Research Initiative Grant (AFOSR FA9550-16-1-0113). The authors thank Dr. Maria T. Dulay for fruitful discussions. The authors thank Prof. Abdullah Sultan from King Fahd University of Petroleum and Minerals, Saudi Arabia, for providing a crude oil sample. Yin-Hung Lai was supported by the Program of Talent Development, Academia Sinica, Taiwan.

#### ■ REFERENCES

- (1) Hashemi, R.; Nassar, N. N.; Pereira Almaso, P. Nanoparticle technology for heavy oil in-situ upgrading and recovery enhancement: Opportunities and challenges. *Appl. Energy* **2014**, *133*, 374–387.
- (2) Rana, M. S.; Samano, V.; Ancheyta, J.; Diaz, J. A. I. A review of recent advances on process technologies for upgrading of heavy oils and residua. *Fuel* **2007**, *86* (9), 1216–1231.
- (3) Carrillo, J. A.; Corredor, L. M. Upgrading of heavy crude oils: Castilla. *Fuel Process. Technol.* **2013**, *109*, 156–162.
- (4) Sahu, R.; Song, B. J.; Im, J. S.; Jeon, Y.-P.; Lee, C. W. A review of recent advances in catalytic hydrocracking of heavy residues. *J. Ind. Eng. Chem.* **2015**, *27*, 12–24.
- (5) Xiu, S. N.; Shahbazi, A. Bio-oil production and upgrading research: A review. *Renewable Sustainable Energy Rev.* **2012**, *16* (7), 4406–4414.
- (6) Crossley, S.; Faria, J.; Shen, M.; Resasco, D. E. Solid Nanoparticles that Catalyze Biofuel Upgrade Reactions at the Water/Oil Interface. *Science* **2010**, *327* (5961), 68–72.
- (7) Brussaard, C. P. D.; Peperzak, L.; Beggah, S.; Wick, L. Y.; Wuerz, B.; Weber, J.; Arey, J. S.; van der Burg, B.; Jonas, A.; Huisman, J.; van der Meer, J. R. Immediate ecotoxicological effects of short-lived oil spills on marine biota. *Nat. Commun.* **2016**, *7*, 11206.
- (8) Gong, Y. Y.; Zhao, X.; Cai, Z. Q.; O'Reilly, S. E.; Hao, X. D.; Zhao, D. Y. A review of oil, dispersed oil and sediment interactions in the aquatic environment: Influence on the fate, transport and remediation of oil spills. *Mar. Pollut. Bull.* **2014**, *79* (1–2), 16–33.
- (9) Yan, T.; Xu, J.; Wang, L. T.; Liu, Y. D.; Yang, C.; Fang, T. A review of upgrading heavy oils with supercritical fluids. *RSC Adv.* **2015**, *5* (92), 75129–75140.
- (10) Kondoh, H.; Tanaka, K.; Nakasaka, Y.; Tago, T.; Masuda, T. Catalytic cracking of heavy oil over  $\text{TiO}_2$ - $\text{ZrO}_2$  catalysts under superheated steam conditions. *Fuel* **2016**, *167*, 288–294.
- (11) Al-Marshed, A.; Hart, A.; Leeke, G.; Greaves, M.; Wood, J. Optimization of Heavy Oil Upgrading Using Dispersed Nanoparticulate Iron Oxide as a Catalyst. *Energy Fuels* **2015**, *29* (10), 6306–6316.
- (12) Kondoh, H.; Hasegawa, N.; Yoshikawa, T.; Nakasaka, Y.; Tago, T.; Masuda, T. Effects of  $\text{H}_2\text{O}$  Addition on Oil Sand Bitumen Cracking Using a  $\text{CeO}_2$ - $\text{ZrO}_2$ - $\text{Al}_2\text{O}_3$ - $\text{FeO}_x$  Catalyst. *Energy Fuels* **2016**, *30* (12), 10358–10364.
- (13) Kwon, S.; Fan, M.; Cooper, A. T.; Yang, H. Q. Photocatalytic applications of micro- and nano- $\text{TiO}_2$  in environmental engineering. *Crit. Rev. Environ. Sci. Technol.* **2008**, *38* (3), 197–226.

- (14) Chen, X.; Liu, L.; Yu, P. Y.; Mao, S. S. Increasing Solar Absorption for Photocatalysis with Black Hydrogenated Titanium Dioxide Nanocrystals. *Science* **2011**, *331* (6018), 746–750.
- (15) Daghbir, R.; Drogui, P.; Robert, D. Modified TiO<sub>2</sub> For Environmental Photocatalytic Applications: A Review. *Ind. Eng. Chem. Res.* **2013**, *52* (10), 3581–3599.
- (16) Yang, H. G.; Sun, C. H.; Qiao, S. Z.; Zou, J.; Liu, G.; Smith, S. C.; Cheng, H. M.; Lu, G. Q. Anatase TiO<sub>2</sub> single crystals with a large percentage of reactive facets. *Nature* **2008**, *453* (7195), 638–641.
- (17) Wu, M. C.; Sapi, A.; Avila, A.; Szabo, M.; Hiltunen, J.; Huuhtanen, M.; Toth, G.; Kukovec, A.; Konya, Z.; Keiski, R.; Su, W. F.; Jantunen, H.; Kordas, K. Enhanced photocatalytic activity of TiO<sub>2</sub> nanofibers and their flexible composite films: Decomposition of organic dyes and efficient H<sub>2</sub> generation from ethanol-water mixtures. *Nano Res.* **2011**, *4* (4), 360–369.
- (18) Garcia-Martinez, M. J.; Da Riva, I.; Canoira, L.; Llamas, J. F.; Alcantara, R.; Gallego, J. L. R. Photodegradation of polycyclic aromatic hydrocarbons in fossil fuels catalysed by supported TiO<sub>2</sub>. *Appl. Catal., B* **2006**, *67* (3–4), 279–289.
- (19) Nair, M.; Luo, Z. H.; Heller, A. Rates of photocatalytic oxidation of crude oil on salt water on buoyant, cenosphere-attached titanium dioxide. *Ind. Eng. Chem. Res.* **1993**, *32* (10), 2318–2323.
- (20) Ireland, J. C.; Davila, B.; Moreno, H.; Fink, S. K.; Tassos, S. Heterogeneous photocatalytic decomposition of polyaromatic hydrocarbons over titanium dioxide. *Chemosphere* **1995**, *30* (5), 965–984.
- (21) Saien, J.; Nejati, H. Enhanced photocatalytic degradation of pollutants in petroleum refinery wastewater under mild conditions. *J. Hazard. Mater.* **2007**, *148* (1–2), 491–495.
- (22) Tang, X. H.; Li, D. Y. Evaluation of Asphaltene Degradation on Highly Ordered TiO<sub>2</sub> Nanotubular Arrays via Variations in Wettability. *Langmuir* **2011**, *27* (3), 1218–1223.
- (23) Ingram, A. J.; Boeser, C. L.; Zare, R. N. Going beyond electrospray: Mass spectrometric studies of chemical reactions in and on liquids. *Chem. Sci.* **2016**, *7* (1), 39–55.
- (24) Fallah-Araghi, A.; Meguellati, K.; Baret, J. C.; El Harrak, A.; Mangeat, T.; Karplus, M.; Ladame, S.; Marques, C. M.; Griffiths, A. D. Enhanced Chemical Synthesis at Soft Interfaces: A Universal Reaction-Adsorption Mechanism in Microcompartments. *Phys. Rev. Lett.* **2014**, *112* (2), 5.
- (25) Espy, R. D.; Wlekinski, M.; Yan, X.; Cooks, R. G. Beyond the flask: Reactions on the fly in ambient mass spectrometry. *TrAC, Trends Anal. Chem.* **2014**, *57*, 135–146.
- (26) Clemett, S. J.; Maechling, C. R.; Zare, R. N.; Swan, P. D.; Walker, R. M. Identification of complex aromatic molecules in individual interplanetary dust particles. *Science* **1993**, *262* (5134), 721–725.
- (27) Mahajan, T. B.; Plows, F. L.; Gillette, J. S.; Zare, R. N.; Logan, G. A. Comparison of microprobe two-step laser desorption/laser ionization mass spectrometry and gas chromatography/mass spectrometry studies of polycyclic aromatic hydrocarbons in ancient terrestrial rocks. *J. Am. Soc. Mass Spectrom.* **2001**, *12* (9), 989–1001.
- (28) Banerjee, S.; Basheer, C.; Zare, R. N. A Study of Heterogeneous Catalysis by Nanoparticle-Embedded Paper-Spray Ionization Mass Spectrometry. *Angew. Chem., Int. Ed.* **2016**, *55* (41), 12807–12811.
- (29) Wu, Q.; Pomerantz, A. E.; Mullins, O. C.; Zare, R. N. Minimization of Fragmentation and Aggregation by Laser Desorption Laser Ionization Mass Spectrometry. *J. Am. Soc. Mass Spectrom.* **2013**, *24* (7), 1116–1122.
- (30) Schlag, E. W. *ZEKE Spectroscopy*; Cambridge University Press: Cambridge, U.K., 1998; p 277.
- (31) Connelly, J. T.; Rolland, J. P.; Whitesides, G. M. "Paper Machine" for Molecular Diagnostics. *Anal. Chem.* **2015**, *87* (15), 7595–7601.
- (32) Wang, H.; Liu, J. J.; Cooks, R. G.; Ouyang, Z. Paper Spray for Direct Analysis of Complex Mixtures Using Mass Spectrometry. *Angew. Chem., Int. Ed.* **2010**, *49* (5), 877–880.
- (33) Pomerantz, A. E.; Hammond, M. R.; Morrow, A. L.; Mullins, O. C.; Zare, R. N. Asphaltene Molecular-Mass Distribution Determined by Two-Step Laser Mass Spectrometry. *Energy Fuels* **2009**, *23*, 1162–1168.
- (34) Linsebigler, A. L.; Lu, G. Q.; Yates, J. T. Photocatalysis on TiO<sub>2</sub> Surfaces: Principles, Mechanisms, and Selected Results. *Chem. Rev.* **1995**, *95* (3), 735–758.
- (35) Hoffmann, M. R.; Martin, S. T.; Choi, W. Y.; Bahnemann, D. W. Environmental applications of semiconductor photocatalysis. *Chem. Rev.* **1995**, *95* (1), 69–96.
- (36) Fenn, J. B. Electrospray wings for molecular elephants (Nobel lecture). *Angew. Chem., Int. Ed.* **2003**, *42* (33), 3871–3894.
- (37) Fox, M. A.; Dulay, M. T. Heterogeneous photocatalysis. *Chem. Rev.* **1993**, *93* (1), 341–357.
- (38) Kebarle, P.; Tang, L. From Ions in Solution to Ions in the Gas Phase: The Mechanism of Electrospray Mass Spectrometry. *Anal. Chem.* **1993**, *65* (22), 972A–986A.
- (39) Li, Y. F.; Yan, X.; Cooks, R. G. The role of the interface in thin film and droplet accelerated reactions studied by competitive substituent effects. *Angew. Chem., Int. Ed.* **2016**, *55* (10), 3433–3437.
- (40) Vargas, R.; Nunez, O. The photocatalytic oxidation of dibenzothiophene (DBT). *J. Mol. Catal. A: Chem.* **2008**, *294* (1–2), 74–81.
- (41) Starks, C. M. Phase-transfer catalysis. I. heterogeneous reactions involving anion transfer by quaternary ammonium and phosphonium salts. *J. Am. Chem. Soc.* **1971**, *93* (1), 195–199.
- (42) Kisch, H. Semiconductor Photocatalysis-Mechanistic and Synthetic Aspects. *Angew. Chem., Int. Ed.* **2013**, *52* (3), 812–847.
- (43) Fujishima, A.; Zhang, X. T.; Tryk, D. A. TiO<sub>2</sub> photocatalysis and related surface phenomena. *Surf. Sci. Rep.* **2008**, *63* (12), 515–582.
- (44) Naeem, K.; Feng, O. Preparation of Fe<sup>3+</sup>-doped TiO<sub>2</sub> nanoparticles and its photocatalytic activity under UV light. *Phys. B* **2010**, *405* (1), 221–226.
- (45) Berry, R. J.; Mueller, M. R. Photocatalytic Decomposition of Crude Oil Slicks Using TiO<sub>2</sub> on a Floating Substrate. *Microchem. J.* **1994**, *50* (1), 28–32.
- (46) Bain, R. M.; Pulliam, C. J.; Cooks, R. G. Accelerated Hantzsch electrospay synthesis with temporal control of reaction intermediates. *Chem. Sci.* **2015**, *6* (1), 397–401.
- (47) Banerjee, S.; Zare, R. N. Syntheses of Isoquinoline and Substituted Quinolines in Charged Microdroplets. *Angew. Chem., Int. Ed.* **2015**, *54* (49), 14795–14799.
- (48) Yan, X.; Bain, R. M.; Cooks, R. G. Organic Reactions in Microdroplets: Reaction Acceleration Revealed by Mass Spectrometry. *Angew. Chem., Int. Ed.* **2016**, *55* (42), 12960–12972.
- (49) Narayan, S.; Muldoon, J.; Finn, M. G.; Fokin, V. V.; Kolb, H. C.; Sharpless, K. B. "On water": Unique reactivity of organic compounds in aqueous suspension. *Angew. Chem., Int. Ed.* **2005**, *44* (21), 3275–3279.